Unsplitting BGK-type Schemes for the Shallow Water Equations

KUN XU

Mathematics Department, Hong Kong University of Science and Technology, Clear Water Bay, Kowloon, Hong Kong

As a continuation of the research on the BGK type schemes, in this paper we present a second order unsplitting method for the shallow water equations. Different from any other approaches, the source terms are included explicitly into the time-dependent flux functions across cell interface.

1 Introduction

The development of unsplitting numerical schemes for the hyperbolic equations with source terms has obtained much attention in recent years [2]. Based largely on the macroscopic equations and wave modelling, it is difficult to develop such kind of schemes. In this paper, for the first time, an unsplitting gas-kinetic scheme for the shallow water equations is developed.

The shallow water equations in 1-D case can be written as

$$W_t + F(W)_x = S(W), \tag{1}$$

where W is the vector of flow variables and $F(W)$ the corresponding fluxes. The source term $S(W)$ accounts for dynamical effects on the flow motion from the wavy river bottom.

If we integrate the above equation in a numerical cell j from $x_{j-1/2}$ to $x_{j+1/2}$, and in a time step from t^n to t^{n+1},

$$\int_{t^n}^{t^{n+1}} \int_{x_{j-1/2}}^{x_{j+1/2}} (W_t + F(W)_x) dx dt = \int_{t^n}^{t^{n+1}} \int_{x_{j-1/2}}^{x_{j+1/2}} S(W) dx dt,$$

we can get

$$W_j^{n+1} - W_j^n = \frac{1}{\Delta x} \int_{t^n}^{t^{n+1}} \left(F_{j-1/2}(t) - F_{j+1/2}(t)\right) dt + \frac{1}{\Delta x} \int_{x_{j-1/2}}^{x_{j+1/2}} \int_{t^n}^{t^{n+1}} S(W) dx dt, \tag{2}$$

where $\Delta x = x_{j+1/2} - x_{j-1/2}$ and W_j is the average value of W in cell j, *i.e.* $W_j = \frac{1}{\Delta x} \int_{x_{j-1/2}}^{x_{j+1/2}} W dx$. The above equation is an exact formulation for a finite-volume scheme.

In order to update W in Eq.(2), a splitting technique is usually used [1], where

$$W_t + F(W)_x = 0 \tag{3}$$

is solved to evaluate the numerical fluxes and $S(W)$ is treated implicitly or explicitly inside each cell. Or, these two stages are coupled using Runge-Kutta methods.

The splitting schemes treat the flow around cell interface and inside each cell differently. Eq.(3) totally ignores the source term effects on the flow motion around cell interface. Physically, the source term never knows where the cell interface is, it definitely effects the flow motion everywhere in space and time. Therefore, the splitting scheme destroys the intrinsic homogeneous of physical space and this distortion can be never eliminated from Runge-Kutta techniques.

As a continuation of previous research [4,5], the focus of this paper is to develop an unsplitting BGK-type scheme for the shallow water equations (Eq.(1)), where the numerical fluxes and source terms are coupled and solved simultaneously in both space and time.

2 Unsplitting BGK Scheme for the Shallow Water Equations

We consider the shallow water equations with source term:

$$\begin{pmatrix} \rho \\ \rho U \end{pmatrix}_t + \begin{pmatrix} \rho U \\ \rho U^2 + \frac{1}{2} G \rho^2 \end{pmatrix}_x = \begin{pmatrix} 0 \\ -H'(x) G \rho \end{pmatrix}. \tag{4}$$

In this system, ρ is the water height, U the velocity, and G the gravitational constant. $H(x)$ is the shape function of river bottom.

The generalized BGK model for the above equation can be constructed as

$$f_t + u f_x = \frac{g - f}{\tau} + s, \tag{5}$$

where f is the gas distribution function and g the equilibrium state f approaches. τ is the particle collision time and s the additional source term.

For the shallow water equations, all f, g and s are functions of space x, time t, and particle velocity u. The equilibrium state g is a Maxwellian

$$g = e^{ln\Pi - \lambda (u-U)^2} = \rho (\frac{\lambda}{\pi})^{\frac{1}{2}} e^{-\lambda (u-U)^2},$$

where $\Pi = \rho(\frac{\lambda}{\pi})^{\frac{1}{2}}$ and λ is related to ρ and G with the relation $\lambda = \frac{1}{\rho G}$. Due to the conservation property in particle collisions, f and g satisfy the compatibility condition

$$\int (f - g) \psi_\alpha du = 0 \qquad \text{for} \qquad \psi_\alpha = (1, u)^T \tag{6}$$

at any points in space and time. The corresponding source term s in Eq.(5) can be constructed as $s = s_1 - s_2$, where

$$s_1 = e^{ln\Pi - \lambda (u + \frac{G}{2} \frac{\partial H}{\partial x})^2} = \rho (\frac{\lambda}{\pi})^{\frac{1}{2}} e^{-\lambda (u + \frac{G}{2} \frac{\partial H}{\partial x})^2}$$

and

$$s_2 = e^{ln\Pi - \lambda(u - \frac{G}{2}\frac{\partial H}{\partial x})^2} = \rho(\frac{\lambda}{\pi})^{\frac{1}{2}} e^{-\lambda(u-\frac{G}{2}\frac{\partial H}{\partial x})^2}.$$

The numerical fluxes for the first term on the right hand side of Eq.(2) are based on the integral solution of the BGK model (Eq.(5)),

$$\begin{aligned} f(x_{j+1/2}, t, u) &= \frac{1}{\tau}\int_0^t (g(x', t', u) + \tau s(x', t', u))\, e^{-(t-t')/\tau} dt' \\ &\quad + e^{-t/\tau} f_0(x_{j+1/2} - ut), \end{aligned} \tag{7}$$

where $x_{j+1/2}$ is the cell interface and $x' = x_{j+1/2} - u(t-t')$ the particle trajectory. There are three unknowns in the above equation. One is the initial gas distribution function f_0 at time $t = 0$. The others are g and s in both space and time locally around $(x_{j+1/2}, t = 0)$. The numerical scheme for solving Eq.(7), along with the compatibility condition(6), is described as follows:

Step(1): Use MUSCL technique to interpolate the conservative variables [3]

$$W_j = (\rho_j, \rho_j U_j)$$

in each cell, and get the reconstructed initial data

$$W_j(x) = W_j(x_j) + \frac{W_j(x_{j+1/2}) - W_j(x_{j-1/2})}{x_{j+1/2} - x_{j-1/2}}(x - x_j) \quad \text{for} \quad x\epsilon[x_{j-1/2}, x_{j+1/2}]. \tag{8}$$

Step(2): Based on the reconstructed data in Step(1), around each cell interface $x_{j+1/2}$, construct the initial gas distribution function f_0,

$$f_0(x) = \begin{cases} g^l\left(1 + a^l(x - x_{j+1/2})\right), & x \le x_{j+1/2} \\ g^r\left(1 + a^r(x - x_{j+1/2})\right), & x \ge x_{j+1/2}, \end{cases} \tag{9}$$

where the states g^l and g^r are the Maxwellian distribution functions which have the one-to-one correspondence to the conservative variables at cell interface;

$$g^l = g^l(W_j(x_{j+1/2})) \qquad \text{and} \qquad g^r = g^r(W_{j+1}(x_{j+1/2})). \tag{10}$$

For example, if we assume

$$g^l = e^{ln\Pi^l - \lambda^l(u-U^l)^2} = \rho^l(\frac{\lambda^l}{\pi})^{\frac{1}{2}} e^{-\lambda^l(u-U^l)^2}, \tag{11}$$

all coefficients in g^l can be obtained as

$$\begin{pmatrix} \rho^l \\ U^l \\ \lambda^l \end{pmatrix} = \begin{pmatrix} \rho_j(x_{j+1/2}) \\ \rho_j U_j(x_{j+1/2})/\rho_j(x_{j+1/2}) \\ 1/(G\rho^l) \end{pmatrix}. \tag{12}$$

Similar equations can be found for g^r. $a^{l,r}$ in Eq.(9) have the forms

$$a^{l,r} = m_1^{l,r} + m_2^{l,r} u + m_3^{l,r} u^2.$$

The coefficients $(m_1^{l,r}, m_2^{l,r}, m_3^{l,r})$ can be determined from $(\rho^l, \rho^l U^l)$ and $(\rho^r, \rho^r U^r)$ and the slopes of the reconstructed mass and momentum in Eq.(8), i.e.

$$\left(\frac{\partial \rho^l}{\partial x}, \frac{\partial (\rho U)^l}{\partial x}\right) \qquad \text{and} \qquad \left(\frac{\partial \rho^r}{\partial x}, \frac{\partial (\rho U)^r}{\partial x}\right).$$

The relations are

$$\begin{aligned} m_1^{l,r} &= \left[(\frac{1}{2\rho} + \frac{3U^2}{G\rho^2}) \frac{\partial \rho}{\partial x} - \frac{2U}{G\rho^2} \frac{\partial (\rho U)}{\partial x} \right]^{l,r} \\ m_2^{l,r} &= \left[-\frac{4U}{G\rho^2} \frac{\partial \rho}{\partial x} + \frac{2}{G\rho^2} \frac{\partial (\rho U)}{\partial x} \right]^{l,r} \\ m_3^{l,r} &= \left[\frac{1}{G\rho^2} \frac{\partial \rho}{\partial x} \right]^{l,r} . \end{aligned} \tag{13}$$

So, all coefficients in Eq.(9) have been obtained from the initially reconstructed data in Step(1). For simplification, we will assume $x_{j+1/2} = 0$ in the rest of this paper.

Step(3): The equilibrium state g is assumed to be continuous across a cell interface

$$g = g_0 \left(1 + (1 - \mathrm{H}[x]) \bar{a}^l x + \mathrm{H}[x] \bar{a}^r x + \bar{A} t\right), \tag{14}$$

where $\mathrm{H}(x)$ is the heaviside function and g_0 the state located at $(x = 0, t = 0)$,

$$g_0 = e^{ln\Pi_0 - \lambda_0 (u - U_0)^2} = \rho_0 (\frac{\lambda_0}{\pi})^{\frac{1}{2}} e^{-\lambda_0 (u - U_0)^2}. \tag{15}$$

$\bar{a}^l, \bar{a}^r$, and $\bar{A}$ in Eq.(14) have the forms

$$\begin{aligned} \bar{a}^{l,r} &= \bar{m}_1^{l,r} + \bar{m}_2^{l,r} u + \bar{m}_3^{l,r} u^2, \\ \bar{A} &= \bar{A}_1 + \bar{A}_2 u + \bar{A}_3 u^2. \end{aligned} \tag{16}$$

Taking both limits $(x \to 0, t \to 0)$ in Eq.(7) and (14), and applying the compatibility condition (Eq.(6)) at $(x = 0, t = 0)$, the macroscopic variables related to g_0 can be uniquely determined in terms of f_0,

$$W_0 = \begin{pmatrix} \rho_0 \\ \rho_0 U_0 \end{pmatrix} = \int g_0 \psi_\alpha du = \int [g^l \mathrm{H}(u) + g^r (1 - \mathrm{H}(u))] \psi_\alpha du, \tag{17}$$

where W_0 is the "averaged " flow variables at the cell interface. Then, connecting W_0 to the cell centered values $W_j(x_j)$ and $W_{j+1}(x_{j+1})$, we can get two slopes for mass and momentum separately

$$\begin{aligned} \left(\frac{\partial \rho_0^l}{\partial x}, \frac{\partial (\rho_0 U_0)^l}{\partial x}\right)^T &= \frac{W_0 - W_j(x_j)}{x_{j+1/2} - x_j} \qquad \text{for} \qquad x \le 0, \\ \left(\frac{\partial \rho_0^r}{\partial x}, \frac{\partial (\rho_0 U_0)^r}{\partial x}\right)^T &= \frac{W_{j+1}(x_{j+1}) - W_0}{x_{j+1} - x_{j+1/2}} \qquad \text{for} \qquad x \ge 0, \end{aligned} \tag{18}$$

from which $(\bar{a}^l, \bar{a}^r)$ can be determined in a similar way as shown in Eq.(13). Now, the only unknown in Eq.(14) is $\bar{A}$, which can be expressed as

$$\bar{A}_1 = \left(\frac{1}{2\rho_0} + \frac{3U_0^2}{G\rho_0^2}\right)\frac{\partial \rho_0}{\partial t} - \frac{2U_0}{G\rho_0^2}\frac{\partial(\rho U)_0}{\partial t},$$

$$\bar{A}_2 = -\frac{4U_0}{G\rho_0^2}\frac{\partial \rho_0}{\partial t} + \frac{2}{G\rho_0^2}\frac{\partial(\rho U)_0}{\partial t},$$

$$\bar{A}_3 = \frac{1}{G\rho_0^2}\frac{\partial \rho_0}{\partial t}, \tag{19}$$

where $\frac{\partial \rho_0}{\partial t}$ and $\frac{\partial(\rho U)_0}{\partial t}$ are unknowns at this time.
Step(4): The source term $(s = s_1 - s_2)$ can be constructed as

$$s_1 = s_{10}\left(1 + (1 - \mathrm{H}[x])\bar{a}^l_{s1}x + \mathrm{H}[x]\bar{a}^r_{s1}x + \bar{A}_{s1}t\right)$$

$$s_2 = s_{20}\left(1 + (1 - \mathrm{H}[x])\bar{a}^l_{s2}x + \mathrm{H}[x]\bar{a}^r_{s2}x + \bar{A}_{s2}t\right), \tag{20}$$

where

$$s_{10} = \rho_0(\frac{\lambda_0}{\pi})^{\frac{1}{2}} e^{-\lambda_0(u+\frac{G}{2}\frac{\partial H}{\partial x})^2},$$

$$s_{20} = \rho_0(\frac{\lambda_0}{\pi})^{\frac{1}{2}} e^{-\lambda_0(u-\frac{G}{2}\frac{\partial H}{\partial x})^2}. \tag{21}$$

$\bar{a}^{l,r}_{s1}$ and $\bar{a}^{l,r}_{s2}$ in Eq.(20) can be written as

$$\bar{a}^{l,r}_{s1} = \bar{\omega}^{l,r}_1 + \bar{\omega}^{l,r}_2 u + \bar{\omega}^{l,r}_3 u^2,$$

$$\bar{a}^{l,r}_{s2} = \bar{\sigma}^{l,r}_1 + \bar{\sigma}^{l,r}_2 u + \bar{\sigma}^{l,r}_3 u^2.$$

The coefficients in the above equations can be easily obtained in terms of $(\rho_0, \rho_0 U_0)$ and their slopes in Eq.(18). For example, for s_1, we have

$$\bar{\omega}^{l,r}_1 = \left[\left(\frac{1}{2\rho_0} + \frac{G}{4\rho_0^2}(\frac{\partial H}{\partial x})^2\right)\frac{\partial \rho_0}{\partial x} - \frac{G}{2\rho_0}\frac{\partial H}{\partial x}\frac{\partial^2 H}{\partial x^2}\right]^{l,r}$$

$$\bar{\omega}^{l,r}_2 = \left[\frac{1}{\rho_0^2}\frac{\partial H}{\partial x}\frac{\partial \rho_0}{\partial x} - \frac{1}{G}\frac{\partial^2 H}{\partial x^2}\right]^{l,r}$$

$$\bar{\omega}^{l,r}_3 = \left[\frac{1}{G\rho_0^2}\frac{\partial \rho_0}{\partial x}\right]^{l,r},$$

and for s_2,

$$\bar{\sigma}^{l,r}_1 = \bar{\omega}^{l,r}_1,$$
$$\bar{\sigma}^{l,r}_2 = -\bar{\omega}^{l,r}_2,$$
$$\bar{\sigma}^{l,r}_3 = \bar{\omega}^{l,r}_3.$$

So, all parameters in Eq.(20) at $t = 0$ have been determined. The unknown terms in (20) are those related to the time derivative of the source terms,

$$\bar{A}_{s1} = \bar{\Omega}_1 + \bar{\Omega}_2 u + \bar{\Omega}_3 u^2$$

and

$$\bar{A}_{s2} = \bar{\Sigma}_1 + \bar{\Sigma}_2 u + \bar{\Sigma}_3 u^2,$$

which are related to $\frac{\partial \rho_0}{\partial t}$,

$$\bar{\Omega}_1 = \left(\frac{1}{2\rho_0} + \frac{G}{4\rho_0^2} (\frac{\partial H}{\partial x})^2 \right) \frac{\partial \rho_0}{\partial t}$$

$$\bar{\Omega}_2 = \frac{1}{\rho_0^2} \frac{\partial H}{\partial x} \frac{\partial \rho_0}{\partial t}$$

$$\bar{\Omega}_3 = \frac{1}{G\rho_0^2} \frac{\partial \rho_0}{\partial t}.$$

Similarly,

$$\bar{\Sigma}_1 = \bar{\Omega}_1$$
$$\bar{\Sigma}_2 = -\bar{\Omega}_2$$
$$\bar{\Sigma}_3 = \bar{\Omega}_3.$$

Step(5): Substitute Eq.(14),(20) and (9) into the integral solution (7), we can obtain the distribution function f at $x = 0$,

$$\begin{aligned} f(0,t,u) &= \gamma_0 \left(g_0 + \tau (s_{10} - s_{20}) \right) \\ &\quad + \gamma_1 \left[\left(\bar{a}^l \mathrm{H}[u] + \bar{a}^r (1 - \mathrm{H}[u]) \right) u g_0 \right. \\ &\quad + \tau \left((\bar{a}^l_{s1} \mathrm{H}[u] + \bar{a}^r_{s1} (1 - \mathrm{H}[u])) u s_{10} - (\bar{a}^l_{s2} \mathrm{H}[u] + \bar{a}^r_{s2} (1 - \mathrm{H}[u])) u s_{20} \right) \Big] \\ &\quad + \gamma_2 \left(\bar{A} g_0 + \tau (\bar{A}_{s1} s_{10} - \bar{A}_{s2} s_{20}) \right) \\ &\quad + \gamma_3 \left((1 - u t a^l) \mathrm{H}[u] g^l + (1 - u t a^r)(1 - \mathrm{H}[u]) g^r \right), \end{aligned} \tag{22}$$

where

$$\gamma_0 = 1 - e^{-t/\tau},$$
$$\gamma_1 = \tau(-1 + e^{-t/\tau}) + t e^{-t/\tau},$$
$$\gamma_2 = \tau(t/\tau - 1 + e^{-t/\tau}),$$
$$\gamma_3 = e^{-t/\tau}.$$

As pointed out in the last two sections, there are two unknowns $(\frac{\partial \rho_0}{\partial t}, \frac{\partial (\rho_0 U_0)}{\partial t})$ in Eq.(22). Since the compatibility condition must be satisfied everywhere in space and time, it can be integrated in a whole CFL time step ΔT at $x = 0$

$$\int_0^{\Delta T} \int \left(f(0,t,u) - g(0,t,u) \right) \psi_\alpha dt du = 0, \tag{23}$$

from which

$$\begin{aligned} (\Gamma_5 \frac{\partial \rho_0}{\partial t}, \Gamma_5 \frac{\partial (\rho U)_0}{\partial t} - \Gamma_2 G \frac{\partial H}{\partial x} \frac{\partial \rho_0}{\partial t})^T &= \int \left[-\Gamma_3 g_0 + \Gamma_1 u \left(\bar{a}^l \mathrm{H}[u] + \bar{a}^r (1 - \mathrm{H}[u]) \right) g_0 \right. \\ &+ \Gamma_3 \left(\mathrm{H}[u] g^l + (1 - \mathrm{H}[u]) g^r \right) \\ &+ \left. \Gamma_4 u \left(a^l \mathrm{H}[u] g^l + a^r (1 - \mathrm{H}[u]) g^r \right) \right] \psi_\alpha du \end{aligned} \tag{24}$$

is obtained. All terms on the right hand side of the above equation are known and

$$\begin{aligned}
\Gamma_0 &= \Delta T - \tau(1 - e^{-\Delta T/\tau}), \\
\Gamma_1 &= \tau\left(-\Delta T + 2\tau(1 - e^{-\Delta T/\tau}) - \Delta T e^{-\Delta T/\tau}\right), \\
\Gamma_2 &= \frac{1}{2}\Delta T^2 - \tau\Delta T + \tau^2(1 - e^{-\Delta T/\tau}), \\
\Gamma_3 &= \tau(1 - e^{-\Delta T/\tau}), \\
\Gamma_4 &= \tau\left(-\Delta T e^{-\Delta T/\tau} + \tau(1 - e^{-\Delta T/\tau})\right), \\
\Gamma_5 &= \tau\left(\Delta T - \tau(1 - e^{-\Delta T/\tau})\right).
\end{aligned}$$

So, $(\frac{\partial\rho_0}{\partial t}, \frac{\partial(\rho_0 U_0)}{\partial t})$ in Eq.(24) can be obtained easily.
Step(6): The time-dependent numerical fluxes of mass and momentum across the cell interface can be obtained using Eq.(22),

$$\begin{pmatrix} F_\rho(t) \\ F_{\rho U}(t) \end{pmatrix}_{j+1/2} = \int u\psi_\alpha f_{j+1/2}(0,t,u)du, \tag{25}$$

from which the time variation of mass density inside each cell j can be evaluated

$$\rho_j(t) = \rho_j(0) + \int_0^t \int u\left(f_{j-1/2}(0,t,u) - f_{j+1/2}(0,t,u)\right) dt du.$$

Since $\rho_j(t)$ is a function of time, the integration of the source term $-H'(x)G\rho$ in a whole time step can be found analytically

$$-H'(x)G\int_0^{\Delta T} \rho_j(t)dt.$$

So, to the second-order of accuracy, both terms on the right hand side of Eq.(2) are obtained from the BGK scheme.

3 Numerical Examples

Two numerical examples for the shallow water equations are presented in this section. The computational domain in both cases is $x\epsilon[0,1]$. The MUSCL limiter is used for interpolations of ρ and ρU in each cell at the beginning of each time step. The time step ΔT is determined using CFL=0.65. The collision time τ is a local constant

$$\tau = \mathcal{C}_1\Delta T\frac{\sqrt{\lambda_0}}{\rho_0} + \mathcal{C}_2\Delta T\frac{|\rho^l\rho^l - \rho^r\rho^r|}{\rho^l\rho^l + \rho^r\rho^r}, \tag{26}$$

where $C_1 = 0.01, C_2 = 1.0$ are fixed in all calculations. The update of flow variables is based on Eq.(2), where the time-dependent flux function $F_{j+1/2}(t)$ and the expicit time integration $S(W_j(t))$ are given at the end of last section.

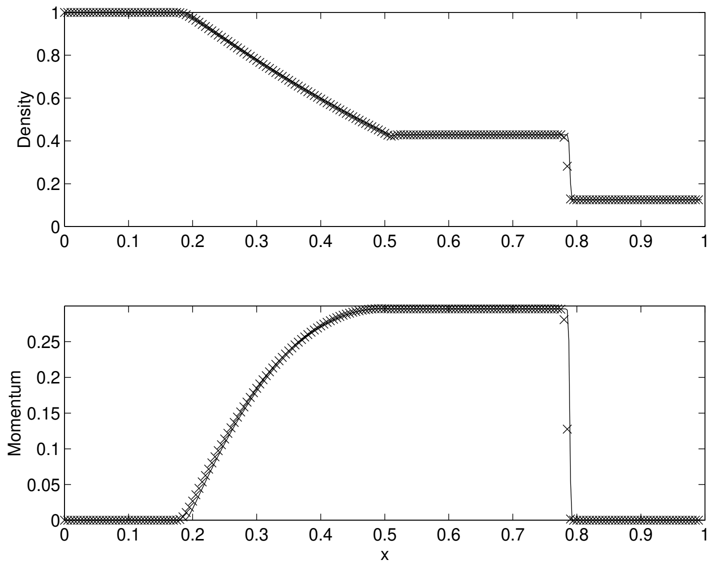

FIGURE 1: Shock Tube Test Case with 200 Points for Shallow Water Equations

In order to validate the scheme, the first test case is a standard shock tube test without source term. The initial condition for this case is

$$(\rho_l = 1.0, U_l = 0.0)|_{x<0.5} \qquad \text{and} \qquad (\rho_r = 0.125, U_r = 0.0)|_{x\geq 0.5}.$$

The simulation results with 200 grid points at time $T = 0.3$ are shown in Fig.(1), where the solid line is the exact solution. From this test case, we can observe that the BGK scheme gives accurate results in both discontinuous and smooth regions.

The second test case is about to study the convergence property of the unsplitting scheme and compare that with the results from splitting scheme. The splitting scheme is different from the unsplitting scheme only in the evaluation of the numerical fluxes, where the homogeneous hyperbolic equations without the source terms (Eq.(3)) are solved. The method for solving the homogeneous equation is also based on the BGK model

$$f_t + u f_x = (g - f)/\tau. \tag{27}$$

The numerical procedures for solving Eq.(27) is the same as that presented in the last section except deleting all terms related to s in step(4) and step(5). As a special case, we are going to test the accuracy of both schemes to keep an exact solution for the shallow water equations and study the convergence property. The shape function of the river bottom is described by the exponential function

$$H(x) = 0.1 e^{\frac{-(x-0.5)^2}{L^2}}$$

where $L = 0.10$. The initial condition is an exact steady state solution of Eq.(4), where the flow variables are

$$\rho = 1 - H(x) \qquad \text{and} \qquad U = 0.$$

In order to keep the above exact solutions ($W_j^{n+1} = W_j^n$), the two terms on the right hand sides of Eq.(2) should compensate each other. However, for the splitting scheme, the flux function $F_{j+1/2}(t)$ does not account for the existence of source term. So, it seems impossible for these two terms to cancel each other accurately. On the other hand, the unsplitting scheme inlcudes source term effects in the flux function, to the second order accuracy both terms should certainly cancel each other partially. Therefore, the unsplitting should have a more accurate solution than that from the splitting scheme. In this case, we have used 17 different cell sizes Δx as shown in Table(1) to study the convergence property in both unsplitting and splitting schemes. The error indicator L_1-norm is defined as

$$L_1 = \frac{\sum_{j=1}^{N} |\rho_j(t) + H(x) - 1|}{N},$$

where N is the total number of cells $N = \frac{1}{\Delta x}$. Although the initial input data is an exact solution, the numerical schemes can not keep this solution. Any schemes will generate artificial waves from wavy bottom region and these errors could propagate throughout the whole computational domain and become background noise as the computational time is long enough. In order to observe both the initial transient and asymptotic behavior of the numerical solution, we have measured the L_1 error at two different output time for both schemes. Some of the computational results are printed in Table(1). Fig.(2) is a plot of the results in a logarithmic scale for the total mesh points N and L_1 error. As indicated from this Figure, the unsplitting scheme almost have consistent errors at both $T = 0.1$ and $T = 1.0$ for different total mesh points, which means that the unsplitting scheme has no obvious initial transient period and it converges to its final asymptotic solution quickly. On the other hand, the splitting scheme takes much longer time to balance both terms on the right hand sides of Eq.(2). It converges slowly to the exact solution, especially at early time $T = 0.1$. In order to get the same accuracy, the splitting scheme needs more than 10 times grid points as that used in unsplitting scheme.

4 Conclusion

In this paper, we have developed the BGK scheme for the shallow water equations with source term. The source term effect are explicitly included in the time-evolution of the gas distribution at a cell interface, from which the numerical fluxes are obtained. The current approach, once again, demonstrates the generality, robustness, and accuracy of the BGK type schemes in solving hyperbolic conservation laws. The scheme presented in this paper, as far as we know, is the first truely unsplitting scheme for the shallow water equations.

TABLE 1: Mesh Refinement Study for Shallow Water Equations

	Unsplitting Scheme		Splitting Scheme	
Δx	L_1 error at T=1.0	L_1 error at T=0.1	L_1 error at T=1.0	L_1 error at T=0.1
$\frac{1}{20}$	1.1453e-4	3.0180e-4	5.3145e-4	2.2799e-3
$\frac{1}{40}$	1.2495e-5	4.1071e-5	9.2667e-5	1.0416e-3
$\frac{1}{60}$	1.9466e-6	1.2897e-5	4.5464e-5	8.1782e-4
$\frac{1}{80}$	5.9010e-7	5.6777e-6	2.5437e-5	4.9959e-4
$\frac{1}{100}$	4.3830e-7	3.0568e-6	1.6832e-5	3.9615e-4
$\frac{1}{150}$	2.5719e-7	1.0550e-6	7.9038e-6	2.6032e-4
$\frac{1}{200}$	1.6143e-7	4.9680e-7	4.7665e-6	1.9454e-4
$\frac{1}{400}$	4.4488e-8	9.3227e-8	1.4835e-6	9.6412e-5
$\frac{1}{800}$	1.1358e-8	2.1318e-8	5.1960e-7	4.7997e-5
$\frac{1}{1600}$	2.8608e-9	5.2739e-9	2.0462e-7	2.3947e-5
$\frac{1}{3200}$	7.3156e-10	1.3293e-9	8.8565e-8	1.1961e-5
$\frac{1}{5000}$	3.1662e-10	5.4678e-10	5.3521e-8	7.6523e-6

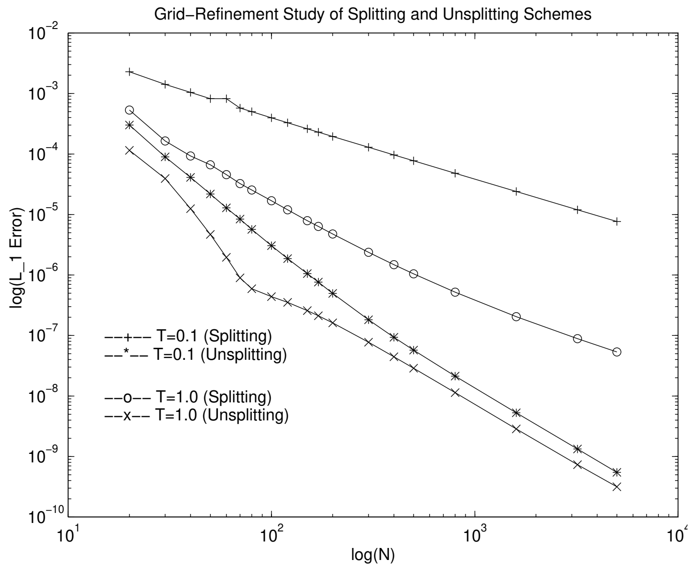

FIGURE 2: Mesh Refinement Study of Unsplitting and Splitting Schemes for Shallow Water Equations

REFERENCES

1. S. Jin, "Runge-Kutta Methods for Hyperbolic Conservation Laws with Stiff Relaxation Terms", J. Comput. Phys., **122**, 51-67, 1995.
2. R.B. Pember, "Numerical Methods for Hyperbolic Conservation Laws with Stiff Relaxation, II. Higher-Order Godunov Methods", SIAM J. Sci. Comput. **14**, No.4, 824-859, 1993.
3. B. van Leer, "Towards the Ultimate Conservative Difference Scheme V. A Second Order Sequel to Godunov's Method", J. of Comput. Phys. **32**, 276-299, 1977.
4. K. Xu, C. Kim, L. Martinelli,and A. Jameson, "BGK-Based Schemes for the Simulation of Compressible Flow" to appear in Int. J. of Comput. Flu. Dyn., 1996.
5. K. Xu, "A Gas-Kinetic Scheme for Hyperbolic Conservation Laws with Source Terms", submitted to J. Comput. Phys., July 1996.